Exosomal αvβ6 integrin is required for monocyte M2 polarization in prostate cancer

Huimin Lu[a,b], Nicholas Bowler[b], Larry A. Harshyne[c], D. Craig Hooper[b,c], Shiv Ram Krishn[a,b], Senem Kurtoglu[a,b], Carmine Fedele[a,b,1], Qin Liu[a,d], Hsin-Yao Tang[e], Andrew V. Kossenkov[e], William K. Kelly[f], Kerith Wang[f], Rhonda B. Kean[b,c], Paul H. Weinreb[g], Lei Yu[h], Anindita Dutta[a,b,2], Paolo Fortina[b,i], Adam Ertel[b,i], Maria Stanczak[j], Flemming Forsberg[j], Dmitry I. Gabrilovich[a,k], David W. Speicher[d,e], Dario C. Altieri[a,k] and Lucia R. Languino[a,b]

a - Prostate Cancer Discovery and Development Program, *Thomas Jefferson University, Philadelphia, Pennsylvania, USA*
b - Department of Cancer Biology, *Sidney Kimmel Cancer Center, Thomas Jefferson University, Philadelphia, Pennsylvania, USA*
c - Department of Neurological Surgery, *Thomas Jefferson University, Philadelphia, Pennsylvania, USA*
d - Molecular and Cellular Oncogenesis Program, *Wistar Institute, Philadelphia, PA, USA*
e - Center for Systems and Computational Biology, *Wistar Institute, Philadelphia, PA, USA*
f - Departments of Medical Oncology, *Sidney Kimmel Cancer Center, Thomas Jefferson University, Philadelphia, PA, USA*
g - Biogen Idec Inc., *Cambridge, MA, USA*
h - Flow Cytometry Core Facility, *Sidney Kimmel Cancer Center, Thomas Jefferson University, Philadelphia, PA, USA*
i - Cancer Genomics and Bioinformatics Laboratory, *Sidney Kimmel Cancer Center, Thomas Jefferson University, Philadelphia, PA, USA*
j - Department of Radiology, *Thomas Jefferson University, Philadelphia, PA, USA*
k - Immunology, *Microenvironment and Metastasis Program, Wistar Institute, Philadelphia, PA, USA*

Correspondence to Lucia R. Languino: *233 S. 10th Street, BLSB 506, Philadelphia, PA 19107, USA. Lucia.Languino@jefferson.edu*
https://doi.org/10.1016/j.matbio.2018.03.009

Abstract

Therapeutic approaches aimed at curing prostate cancer are only partially successful given the occurrence of highly metastatic resistant phenotypes that frequently develop in response to therapies. Recently, we have described αvβ6, a surface receptor of the integrin family as a novel therapeutic target for prostate cancer; this epithelial-specific molecule is an ideal target since, unlike other integrins, it is found in different types of cancer but not in normal tissues.

We describe a novel αvβ6-mediated signaling pathway that has profound effects on the microenvironment. We show that αvβ6 is transferred from cancer cells to monocytes, including β6-null monocytes, by exosomes and that monocytes from prostate cancer patients, but not from healthy volunteers, express αvβ6. Cancer cell exosomes, purified via density gradients, promote M2 polarization, whereas αvβ6 down-regulation in exosomes inhibits M2 polarization in recipient monocytes. Also, as evaluated by our proteomic analysis, αvβ6 down-regulation causes a significant increase in donor cancer cells, and their exosomes, of two molecules that have a tumor suppressive role, STAT1 and MX1/2. Finally, using the *Pten*$^{pc-/-}$ prostate cancer mouse model, which carries a prostate epithelial-specific Pten deletion, we demonstrate that αvβ6 inhibition in vivo causes up-regulation of STAT1 in cancer cells.

Our results provide evidence of a novel mechanism that regulates M2 polarization and prostate cancer progression through transfer of αvβ6 from cancer cells to monocytes through exosomes.

Introduction

Prostate cancer is one of the leading causes of cancer-related deaths among men in the United States [1]. The disease has heterogeneous growth patterns, and its prognosis is poor when it becomes metastatic [2] or androgen-independent (castrate-resistant prostate cancer, CRPC), which remains incurable with elevated morbidity and mortality. These features highlight the pressing urgency for a better mechanistic understanding of pathways of prostate cancer progression [3,4].

Signaling mediated by the integrin family of cell adhesion receptors has been implicated as a mechanistic driver of this disease [5–8]. Integrins are transmembrane cell adhesion receptors that are comprised of one α and one β subunit; these molecules play a key role in cellular homeostasis in normal tissues, and become de-regulated in a variety of epithelial malignancies, including prostate cancer progression to advanced disease stages [9–12], where they promote cell survival, adhesion, proliferation, and modulation of invasive phenotypes [6,10]. In particular, the epithelial-specific αvβ6 integrin, not detectable in the normal prostate of humans or mice, is expressed at high levels in cancer [13,14]. Taken together, these results support a pivotal role of αvβ6 as an important therapeutic target in advanced prostate cancer. Another αv-containing integrin, αvβ3, present in normal prostate at low levels, is up-regulated in primary and metastatic prostate cancer [9,10,15], but unlike αvβ6, αvβ3 promotes osteoblastic metastasis [16]. The αvβ6 integrin is localized in focal contacts, and functionally, mediates adhesion to fibronectin as well as latency associated peptide (LAP)-TGFβ1, promoting the release of active TGFβ1, which functions as a pro-metastatic cytokine [17], as well as an osteolytic program in prostate cancer cells [18]. The αvβ6 integrin promotes tumor growth in vivo as shown by others and us and is shown to be a therapeutic target in breast cancer and prostate cancer [14,19]. Finally, αvβ6 correlates with poor survival in breast [19], cervical [20] and colorectal [21] cancer.

Very recently, we and others have shown that integrins, which are transmembrane glycoproteins deregulated in cancer [5,9,22], as well as other bioactive molecules, basement membrane assembly [23] or specific subunits partaking in a number of diverse of key roles [24–28] are found in extracellular vesicles (EVs), including exosomes. These EVs mediate interactions between the tumor, tumor microenvironment (TME) and extracellular matrix (ECM). Specifically, we have published that the αvβ6 integrin is transferred from cancer cells to recipient cells via exosomes and remains active in these cells [29]. Exosomes are small (50–150 nm) EVs present in blood, urine and the medium of cultured cells [30], different from oncosomes also found in prostate cancer [31,32]. The field of exosome research is a fast growing area of investigation, and in the past decade exosomes have emerged as important mediators of intercellular communication, frequently involved in malignancy [29,33]. Exosomes have been shown in the serum of patients harboring a variety of tumors, correlating with advanced disease stages; their number in human blood is very abundant with specific subsets increased in cancer [34]. There is evidence that exosomes released from cancer cells promote a pro-metastatic phenotype through extracellular matrix remodeling [35,36], and a potential role of integrins packaged in tumor-released exosomes, in mediating advanced disease traits, has only recently begun to emerge [33,37]. Given the failure of ipilimumab (an antibody that binds CTLA4) to improve survival in prostate cancer patients and the paucity of T cells in prostate cancer tissues [38], recent work has begun to investigate the possibility that macrophages may be key players in prostate cancer progression. In cancer, macrophages can exert both anti- and pro-tumoral functions. Macrophages are heterogeneous cells with high plasticity representing a wide spectrum of activation states, ranging from the classically activated M1 macrophages to several subsets of alternatively activated M2 macrophage. Anti-inflammatory M2 macrophages are better adapted to scavenging debris and releasing growth factors that promote angiogenesis and fibrosis [39]. Even still highly phagocytic, the major role of M2 macrophages is helping with repair of injuries by engulfing cell debris, regulating tissue re-modeling, and promoting normal cell turnover [40]. ECM pathways mediate M2 polarization, as shown in kidney whereby homogenization of renal ECM structure induces instead M1 macrophage polarization suggesting an important role of the 3D architecture [41].

Activation to M2 macrophages can occur through a variety of signals, including those mediated by cytokines including IL-4, IL-10, IL-13 and TGFβ, and can be promoted by the presence of glucocorticoid hormones [42]. Tumor-associated macrophages (TAMs) are the major component of the immune infiltrate of the stroma of solid tumors, representing up to 50% of the tumor mass where they can play a key role in tumor development [43,44]. TAMs are evidently educated by the TME in that they generally acquire the hallmarks of M2 macrophages, with their associated anti-inflammatory, immune modulatory, and angiogenic properties that promote tissue remodeling [45]. Different subsets of M2 macrophages produce IL-10, TGFβ, VEGF as well as various combinations of certain factors more often associated with a classical pro-inflammatory M1 macrophage subset. Among the M2 phenotypic markers shared by TAM are the scavenger receptors CD163, CD204, CD206, and Arg-1 as well as classical macrophage markers. A team led by Dr. Pienta has promoted the

Please cite this article as: H. Lu, et al., Exosomal αvβ6 integrin is required for monocyte M2 polarization in prostate cancer, Matrix Biol (2017), https://doi.org/10.1016/j.matbio.2018.03.009

idea that macrophages support prostate cancer tumorigenicity via CCL2, a chemokine known to recruit monocytes and macrophages to sites of inflammation in tumor beds [46].

Our data demonstrate that αvβ6 has profound effects on the TME. Specifically, we show that αvβ6 prevents the induction of the STAT1/MX1/2 signaling pathway in cancer cells and their exosomes, and that its down-regulation or inhibition in vivo in cancer exosomes inhibits the polarization of monocytes toward a M2 phenotype and causes up-regulation of the M2 inhibitor interferon-γ pathway. This study indicates that inhibition of this integrin and its downstream effectors might offer a novel immune – based therapeutic strategy in prostate cancer.

Results

αvβ6-positive cancer cell exosomes are transferred to peripheral blood mononuclear cells (PBMC)

We have previously shown that the αvβ6 integrin is shed by prostate cancer cells packaged in EVs which, in turn, transfer this integrin to recipient αvβ6 negative cancer cells [29]. We hypothesized that this transfer to αvβ6 negative cells in the microenvironment amplifies the signals mediated by αvβ6 in the tumor. To test this hypothesis, we selected peripheral blood mononuclear cells (PBMC) as recipient cells due to their content of monocytes, the precursors of

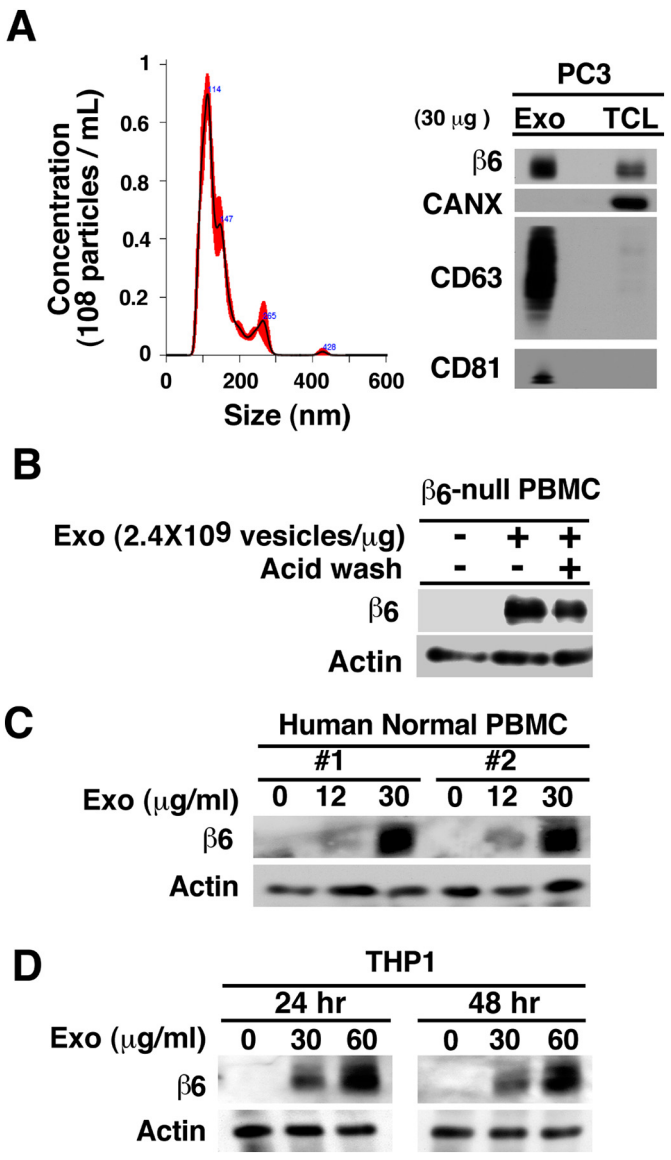

Fig. 1. Exosomal αvβ6 is transferred from prostate cancer cells to PBMC. (A), Left, nanoparticle size distribution analysis of PC3 exosomes (Exo) by NTA. Right, IB analysis of β6 integrin, exosomal markers CD63, CD81 and calnexin (CANX) in lysates of PC3 Exo and cells (TCL). (B), PBMC (3.0×10^5 cells) derived from β6-null mice (pool of 3 mice) were incubated with PC3 Exo (30 μg/mL at a concentration of 2.4×10^9 vesicles/μg) for 24 h. The cells were washed with acid wash buffer twice followed by IB analysis of cell lysates for expression of β6 integrin and actin (loading control). (C), PBMC (3.0×10^5 cells) from two different human healthy donors were incubated with indicated PC3 Exo concentrations (0, 12, 30 μg/mL at a concentration of 2.4×10^9 vesicles/μg) for 24 h and cell lysates were analyzed by IB for expression of β6 integrin and actin (loading control). (D), THP1 cells (3.0×10^5 cells) were incubated with the indicated PC3 Exo concentrations (0, 30, 60 μ/mL at a concentration of 2.4×10^9 vesicles/μg) for 24 and 48 h and analyzed by IB for expression of β6 integrin and actin (loading control).

Please cite this article as: H. Lu, et al., Exosomal αvβ6 integrin is required for monocyte M2 polarization in prostate cancer, Matrix Biol (2017), https://doi.org/10.1016/j.matbio.2018.03.009

TAM. We first purified EVs from PC3 cells by differential centrifugation at 100 K*g* as previously described [47]; then, characterized the EV using the following approaches: NTA, which confirmed that the majority of the EVs have a size of 130–150 nm; immunoblotting (IB), which shows the characteristic exosomal enrichment in CD63 and CD81 (Fig. 1) and by iodixanol density gradient separation (Fig. 2). Therefore, the isolated EVs are designated exosomes in our study. Routine IB analysis also shows that these exosomes do not express calnexin (CANX), an endoplasmic reticulum (ER) marker (Fig. 1A).

We incubated PC3 cell exosome preparations with PBMC isolated from β6-null mice (Fig. 1B). The PBMC, isolated from β6-null mice were 5.58% monocytes and 88.4% lymphocytes. The majority of the gated monocytes are CD11b-positive (Fig. S1). The results obtained using PBMC from β6-null mice (Fig. 1B) show that β6 is transferred to these cells and confirm that the expression of β6 integrin in the PBMC is not the result of endogenous β6 integrin synthesis. Furthermore, the results show that acid wash only slightly reduced β6 levels transferred to PBMC, indicating that the newly detected αvβ6 levels are not due to exosome attachment to the cell surface. Finally, we tested whether PBMC from two healthy donors or THP1 cells would express β6 integrin upon incubation with exosomes isolated from PC3 cells. The results show that β6 is transferred to PBMC isolated from healthy donors ($n = 5$, Fig. 1C) and THP1 cells (Fig. 1D). The results also show that exosome transfer to PBMC occurs in a concentration-dependent manner and reaches a plateau at 24 h. Furthermore, we transfected β6-

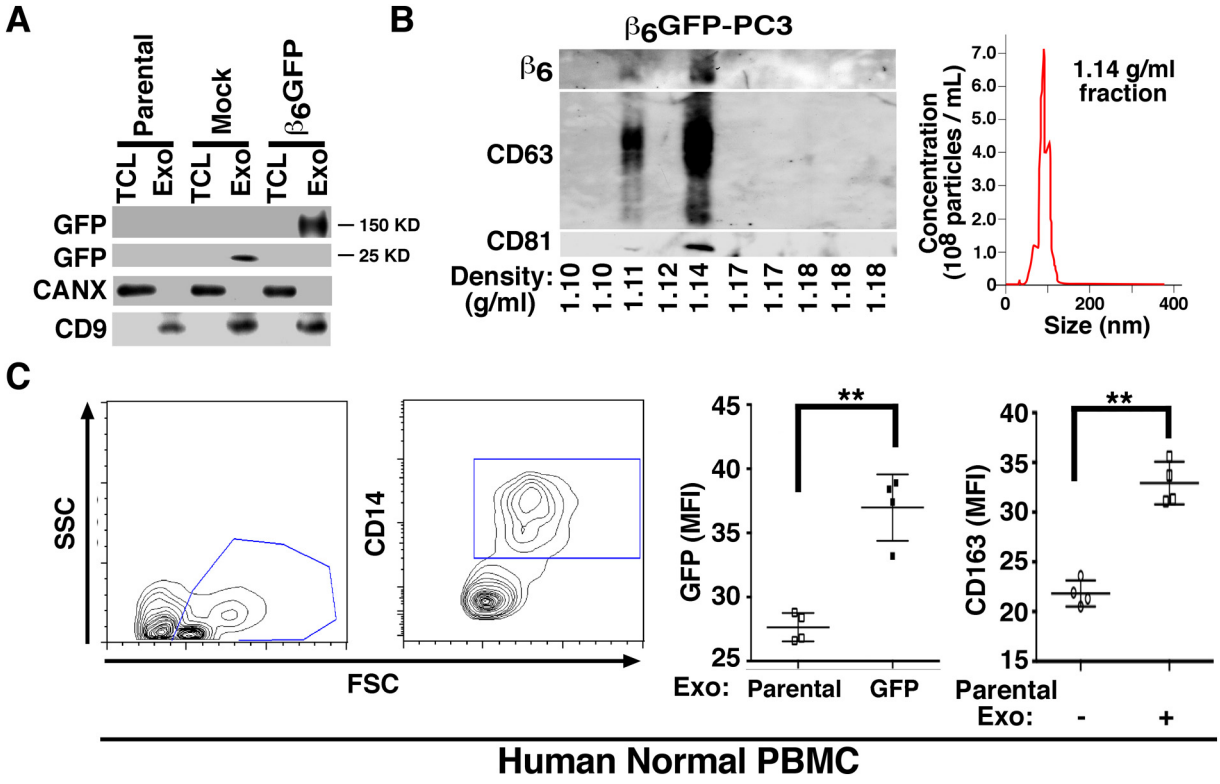

Fig. 2. Transfer of GFP-tagged αvβ6 integrin to PBMC. (A), IB analysis for expression of GFP, CANX and exosomal marker CD9 in parental PC3, EGFP-PC3 (Mock) and β6-EGFP-PC3 derived exosome lysate (Exo) and total cell lysate (TCL). (B), Left, Iodixanol gradient analysis of β6-EGFP-PC3 derived Exo was performed as described in the Experimental Procedures. Expression of β6, CD63, and CD81 analyzed by IB is shown. The expected density range for Exo is 1.11–1.14 g/mL. Right, NTA for the fifth fraction (density 1.14 g/mL) from the iodixanol gradient of β6-EGFP-PC3 derived Exo is shown. (C), Left, human normal PBMC (2.0×10^5 cells) incubated with 8 μg/mL of β6-EGFP-PC3 Exo for 36 h, were immuno-stained for CD14. Flow cytometric contour plots of cells gated as $CD14^+$ monocytes are shown. Middle, flow cytometric analysis of comparative expression of GFP measured as mean fluorescence intensity (MFI) in PBMC incubated with parental PC3 or β6-EGFP-PC3 Exo (8 μg/mL for 36 h). Right, flow cytometric analysis of comparative expression of CD163 (M2 macrophage marker) measured as MFI in PBMC incubated with or without parental PC3 (8 μg/mL for 36 h). Two graphs showing GFP and CD163 MFI include data from 4 biological replicates tested in 2 different experiments. **: $p < 0.01$, student's *t*-test.

Please cite this article as: H. Lu, et al., Exosomal αvβ6 integrin is required for monocyte M2 polarization in prostate cancer, Matrix Biol (2017), https://doi.org/10.1016/j.matbio.2018.03.009

EGFP into PC3 cells and isolated exosomes from these cells first by differential centrifugation at 100 K*g* [29,48] and then by iodixanol gradient separation. The preparations obtained by differential centrifugation at 100 K*g* do not express CANX whereas they express CD9 (Fig. 2A); the fused β6-EGFP is detected at 150 KD, while the EGFP is at 25 KD. The αvβ6 positive exosomes, purified on an iodixanol density gradient, contain the exosomal markers CD63 and CD81 in fraction 5 (density = 1.14 g/mL) and have an average size of 100 nm (Fig. 2B). Finally, we incubated these purified exosomes with human PBMC isolated from two healthy donors and then, characterized the cells by FACS for CD14, GFP and CD163 expression (Fig. 2C). Our FACS analysis shows that GFP-β6 is found in CD14-positive PBMC upon exosome incubation (Fig. 2C), but not in CD14-negative cells (data not shown). Overall, these results show that exosomal β6, shed by cancer cells, is transferred to CD14-positive monocytes and is associated with their expression of CD163.

αvβ6 down-regulation in cancer cell exosomes inhibits M2 polarization of PBMC

The fact that CD14-positive PBMC acquire αvβ6 and CD163 upon incubation with exosomes containing this integrin, led us to further examine the effect of the exosomes on monocyte differentiation, particularly since M2 polarization is known to promote tumor growth [43,44,49]. To more specifically demonstrate that αvβ6 contributes to M2 polarization, we down-regulated αvβ6 in the PC3 cells using siRNA, and isolated exosomes from these cells for treatment of human normal PBMC. We used 4 different groups of PC3 cells, which were either not incubated (–) or incubated with the following siRNA: non-silencing (NS), or β6 integrin targeting siRNAs (D1 or D2) [14,18,29]. A significantly lower percentage of CD14 gated-CD163+/CD204+ cells is observed upon incubation of exosomes isolated from αvβ6 down-regulated cells (7% vs. 35%) (Fig. 3A). Fig. 3B shows that the expression of M2 polarization

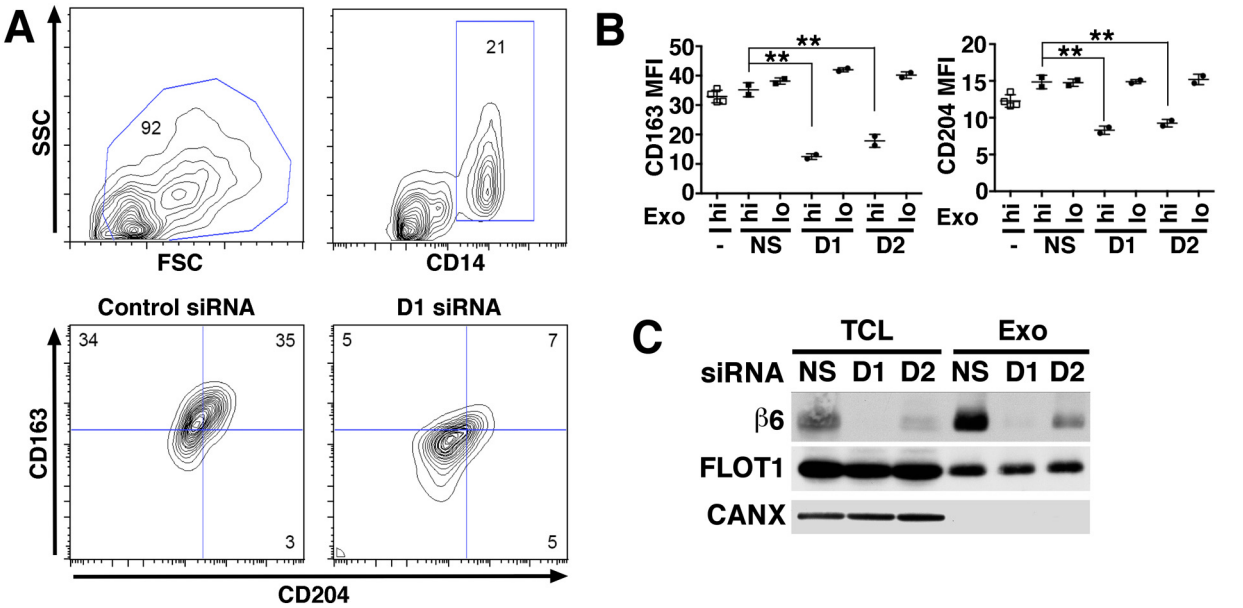

Fig. 3. αvβ6 integrin down-regulation in exosomes inhibits recipient monocyte M2 differentiation. Human PBMC (2.0×10^5 cells) derived from two healthy donors were incubated for 48 h with different concentrations of exosomes (Exo) (hi: 8 μg/mL; lo: 0.8 μg/mL) derived from PC3 cells incubated with no siRNA, a non-silencing siRNA (NS) or with one of two different siRNAs specific to β6 mRNA (D1 or D2). Cultures were harvested at 48 h for M2 monocyte polarization analysis by flow cytometry. (A), Contour plots depict live gating of $CD14^+$ monocytes and representative expression of M2 polarization markers CD163 and CD204 in this population. Numbers indicate the percentage of gated cells. (B), There are 4 different PBMC treatment groups: untreated cells (–); NS, PBMC treated with exosomes from PC3 cells transfected with non-silencing siRNA; D1, PBMC treated with exosomes from PC3 cells transfected with a β6-siRNA duplex designated D1; D2, PBMC treated with exosomes from PC3 cells transfected with a different β6-siRNA designated D2. Mean fluorescence intensity (MFI). The percentages of CD14 gated CD163+/CD204+ cells in D1-hi, and D2-hi are statistically lower than NS, as assessed by Dunnett's test. **: $p < 0.01$. (C), IB analysis of β6 integrin expression in TCL and Exo derived from PC3 cells transfected with NS siRNA or with β6 siRNA (D1 and D2). Flotilin 1 (FLOT1) was used as loading control for TCL and Exo, whereas CANX was used as loading control for TCL but not Exo.

Please cite this article as: H. Lu, et al., Exosomal αvβ6 integrin is required for monocyte M2 polarization in prostate cancer, Matrix Biol (2017), https://doi.org/10.1016/j.matbio.2018.03.009

specific markers, CD163 and CD204 in normal CD14-positive PBMC is moderately increased by incubation with αvβ6 bearing exosomes isolated from PC3 cells transfected with a non-silencing siRNA. In contrast, treatment of the CD14-positive PBMC with exosomes from siRNA treated PC3 cells in which αvβ6 expression has been down-regulated, significantly reduces CD163 and CD204 expression. Similar results are obtained using either D1 or D2 siRNAs, two different duplexes targeting β6-integrin [14,18]. IB analysis shows an enrichment of β6 in exosomes as compared to TCL in non-silencing controls, while a significant reduction is observed in both TCL and exosomes upon β6 siRNA treatment (Fig. 3C). The exosome preparations utilized lack CANX (Fig. 3C).

Down-regulation of the αvβ6 integrin in PC3 cells affects the exosomal proteome composition

We performed an extensive proteomic analysis of PC3 exosome lysates. We purified exosomes from these same 4 groups of cells described above and performed a comparative label-free proteomic analysis (2037 proteins). Unsupervised hierarchical clustering of protein intensities demonstrates dramatic differences between exosome proteomes (Fig. 4A) using exosomes from non-treated cells (NT) and cells treated with NS siRNA clustering together, while exosomes from cells treated with either D1 or D2 siRNA cluster together. Overall, 339 proteins are significantly affected by β6 integrin down-regulation (FDR < 10%) with the majority of them being up-regulated in exosomes ($n = 239$, 79.7%).

The changes in protein abundance within exosomes are emphasized in our focused analysis shown in Fig. 4B. In order to find proteins most affected by the β6 integrin knockdown, we selected only robustly detected candidates (at least 10 MS/MS counts, 10 unique peptides) that significantly changed (FDR < 10%) at least 4 fold. In-depth analysis shows that many signaling molecules from the interferon-γ pathway which blocks M2 in favor of M1 monocyte polarization such as STAT1, MX1, and MX2 are increased upon β6 integrin down-regulation. In fact, among all 239 proteins upregulated upon αvβ6 knockdown, we find a significant enrichment of proteins involved in interferon signaling (14 proteins,

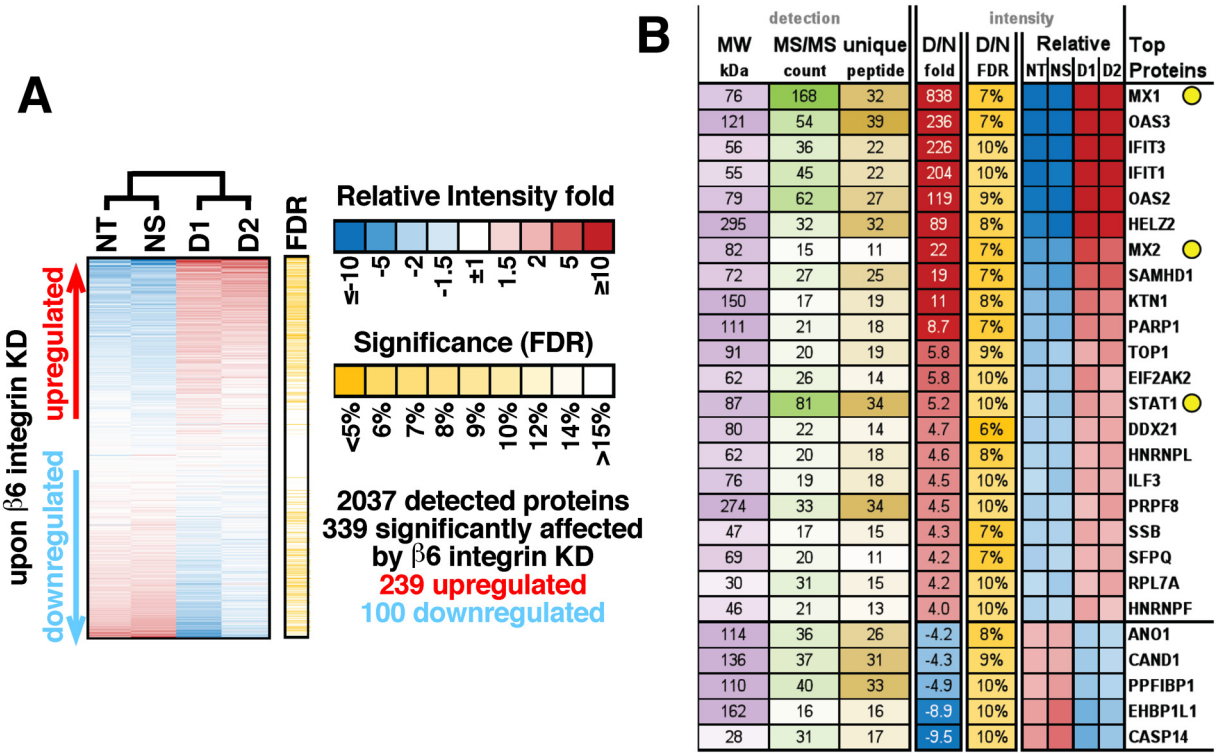

Fig. 4. Proteomics analysis of Exosomes from PC3 cells upon β6 integrin knockdown reveals increased expression of STAT1 and MX1/2 proteins. (A) Results of a proteomics experiment comparing exosomes from non-treated cells (NT), cells treated with non-silencing siRNA (NS), or two β6 integrin siRNAs (D1 and D2). Unsupervised hierarchical clustering based on label-free quantification of protein intensities is shown. Each horizontal bar is a unique protein and a total of 2037 proteins are shown in this heat map. Red = higher, blue = lower protein abundance. (B) Heatmap of relative protein levels for the proteins most significantly affected by D1 and D2, detected with at least 10 MS/MS counts and 10 unique peptides.

Please cite this article as: H. Lu, et al., Exosomal αvβ6 integrin is required for monocyte M2 polarization in prostate cancer, Matrix Biol (2017), https://doi.org/10.1016/j.matbio.2018.03.009

26 fold more than expected by chance, $p = 1 \times 10^{-10}$ by Fisher Exact test). MX1 levels are the most affected followed by MX2 and STAT1; they increased respectively: 838 fold, 22 and 5.2 fold. Enrichment of STAT1 in PC3 exosomes in which αvβ6 has been down-regulated appears to be specific since the levels of EGFR, another molecule known to activate STAT1 [50], do not show significant up-regulation (down-regulated 1.4 fold, $p = 0.094$). In contrast, Protein inhibitor of activated STAT1 (PIAS1), which inhibits STAT1-mediated gene activation [51] and is increased in prostate cancer [52], is detected in cells but not in exosomes, although the levels were not changed upon αvβ6 down-regulation.

STAT1 levels in cells and exosomes increase upon αvβ6 integrin down-regulation

The proteomic results were validated by IB analysis and show that STAT1 accumulates in cells and consequently in exosomes upon down-regulation of β6 by siRNA (Fig. 5A and B); and that MX1/2 accumulates just in exosomes upon down-regulation of β6 (Fig. 5C). TSG101 (Fig. 5A, bottom), CD81, CD63 (Fig. 5B) and CD9 (Fig. 5B and C) are used as exosomal markers, whereas ERK (Fig. 5A, top) and CANX (Fig. 5B and C) are used as loading controls for TCL. As expected, the levels of CD81, CD9 and CD63 are highly enriched in the exosome preparations as compared to TCL. The absence of CANX in the exosome preparations confirms the purity of the isolated exosome fractions (Fig. 5C).

The results in Fig. 5C indicate that packaging of STAT1 into exosomes is likely a reflection of increased STAT1, but not MX1/2, levels in the cells. However, the proteomic results were also validated by IB analysis upon blocking of β6 by 6.3G9 a monoclonal antibody (mAb) to αvβ6 and show that STAT1 and MX1/2 accumulate in cells (Fig. 6A). The 6.3G9 Ab does not affect cell viability of prostate epithelial cells, however, it does inhibit prostate cell adhesion ([14] and data not shown).

These results obtained in vitro were validated in vivo. We reported previously that αvβ6 is required for prostate cancer growth in non-castrated and castrated *Pten*$^{pc-/-}$ mice, a well-established prostate cancer model [14]. The tumor size was measured by ultrasound before Ab injection. The average volume of the tumor is 18.9 mm^3 in 6.3G9 group, compared with 18.2 mm^3 in 1E6 group, the isotype control mAb; *t*-test shows no significant difference in tumor sizes between the 6.3G9 and 1E6 groups (data not shown). Administration of 6.3G9, to *Pten*$^{pc-/-}$ mice results in acute disruption of epithelial layers of prostate adenocarcinoma and in a significant decrease in tumor weight as compared with mice treated with 1E6. In our previous study, 6.3G9 did not show disruption of epithelial layers in normal glands

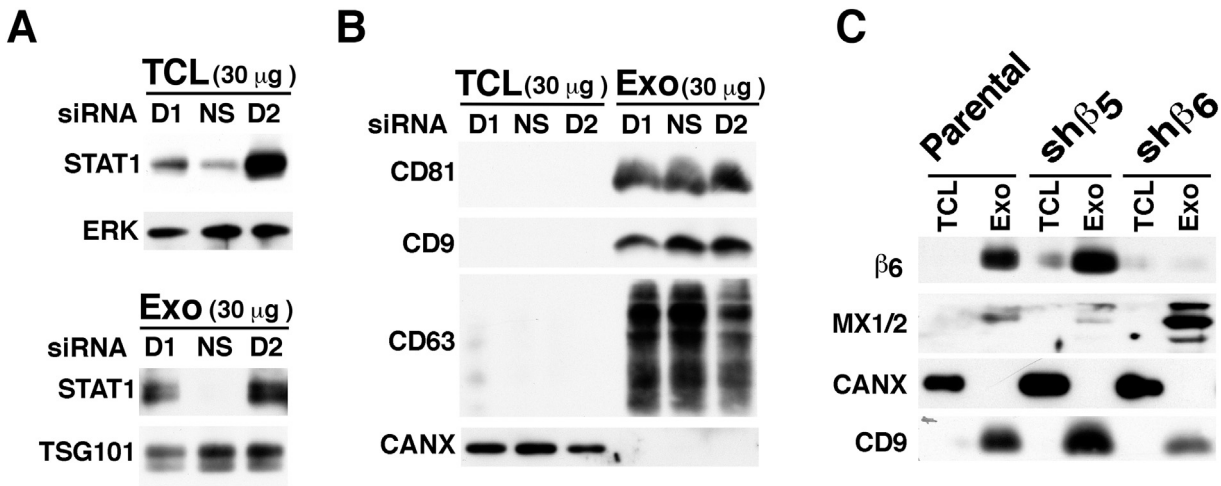

Fig. 5. β6 integrin down-regulation results in increased expression of STAT1 and MX1/2 in PC3 cells and exosomes. (A), IB analysis of STAT1 expression in 30 μg of exosome lysate (Exo) and total cell lysate (TCL) derived from PC3 cells incubated either with a non-silencing siRNA (NS siRNA) or with β6 mRNA directed siRNA (D1 or D2). ERK was used as loading control for TCL and TSG101 was used as loading control for Exo lysate. (B), IB analysis of the expression of exosomal markers CD81, CD9, CD63 in PC3 cell Exo lysate and TCL derived from PC3 cells incubated either with a NS siRNA or with D1 and D2 siRNA. CANX was used as loading control found in TCL but not in Exo. (C), IB analysis of the expression of β6 integrin and MX1/2 in TCL and Exo derived from parental PC3 cells or PC3 cells transfected with shβ6 or shβ5 retroviral constructs. PC3-shβ5 transfectants are used as a negative control. CANX was used as a loading control for TCL and CD9 was used as a loading control for Exo lysates.

Please cite this article as: H. Lu, et al., Exosomal αvβ6 integrin is required for monocyte M2 polarization in prostate cancer, Matrix Biol (2017), https://doi.org/10.1016/j.matbio.2018.03.009

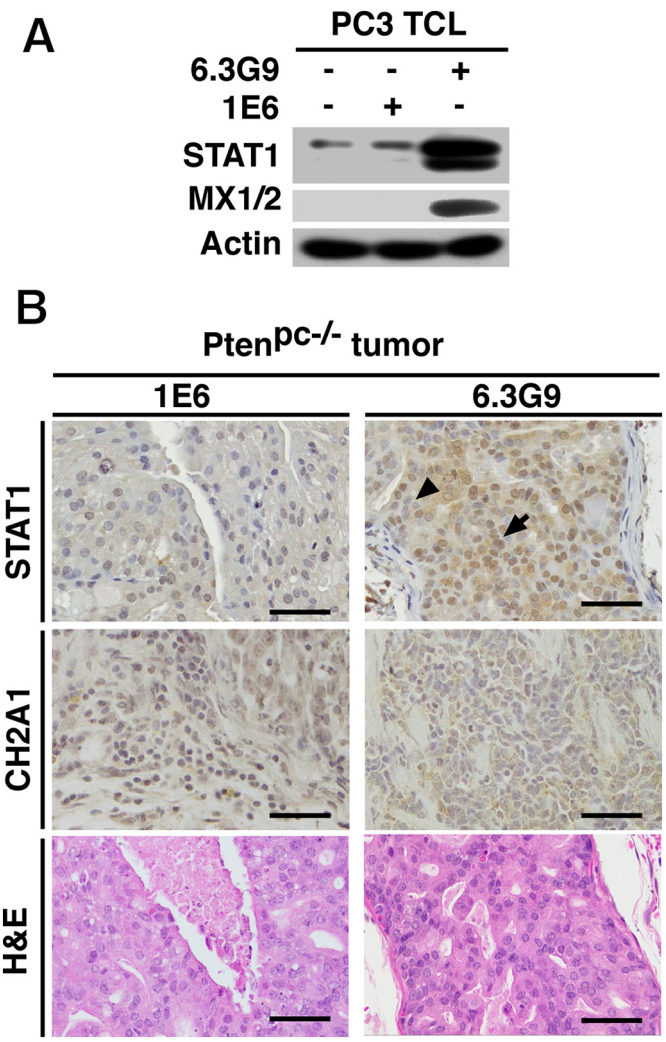

Fig. 6. Inhibition of αvβ6 increases STAT1 levels in prostate cancer cells and *Pten*$^{pc-/-}$ mice. (A), Evaluation of STAT1 and MX1/2 levels by IB in TCL from PC3 cells either untreated or treated with αvβ6 monoclonal antibody 6.3G9 or isotype control antibody 1E6 (both at 10 μg/mL). Actin was used as loading control. (B), Immunohistochemical analysis of STAT1 and αvβ6 expression in prostate tumors from *Pten*$^{pc-/-}$ mice (sacrificed at 10–13 weeks) treated with 6.3G9 or 1E6 antibodies (10 mg/K*g*/week × 5 weeks; $n = 5$). Representative IHC and H&E images are shown (Scale bar, 100 μm). Arrow, STAT1 expression in nuclei of prostate tumor cells. Arrowhead, nuclei of prostate tumor cells lacking STAT1 expression.

[14]. In the current study, using *Pten*$^{pc-/-}$ mice treated with an Ab to αvβ6, 6.3G9, or 1E6, we show that STAT1 accumulates in the αvβ6 expressing cancer cells (Fig. 6B). In the 6.3G9 treated tumors, 65.1% malignant cells show STAT1 staining versus only 17.9% in the 1E6 treated tumors (Fig. 6B).

To analyze the relevance of our observation that an epithelial specific integrin, αvβ6, is transferred to monocytes, we studied whether αvβ6 is expressed in vivo in monocytes from cancer patients or tumor-bearing mice. We first tested αvβ6 expression in PBMC isolated from whole blood using the Lympholyte density gradient from 14 prostate cancer patients (including 8 CRPC patients). As control, PBMC from 5 healthy donors were used. The results in Fig. 7A show a representative flow analysis. Expression of αvβ6 is found in monocytes from 9 out of 14 prostate cancer patients, and 6 out of the 8 CRPC patients, but not in monocytes from healthy donors or lymphocytes from either prostate cancer patients or healthy donors.

We then studied whether αvβ6 is expressed in monocytes from tumor-bearing mice; as control, PBMC from normal mice were used. For this analysis, we tested αvβ6 expression in PBMC isolated from whole blood using the Lympholyte density gradient from 11 *Pten*$^{pc-/-}$ mice, and 9 Pten wild-type mice (Fig. S2). Expression of αvβ6 is not found in monocytes from normal mice although its expression levels are variable (Fig. S2). As observed in human PBMC, αvβ6 is not detectable in lymphocytes from *Pten*$^{pc-/-}$ or wild-type mice, suggesting a monocyte specific uptake of the αvβ6 exosomes.

In conclusion, based on our results, the model proposed here in Fig. 7B is as follows: αvβ6-positive or αvβ6-negative exosomes are released by cancer cells and transferred to monocytes, thus respectively supporting or, rather, preventing M2 polarization in favor of M1 macrophage polarization. Consequently, by down-regulating or inhibiting αvβ6 in cancer cells, we expect that increased STAT1/

Please cite this article as: H. Lu, et al., Exosomal αvβ6 integrin is required for monocyte M2 polarization in prostate cancer, Matrix Biol (2017), https://doi.org/10.1016/j.matbio.2018.03.009

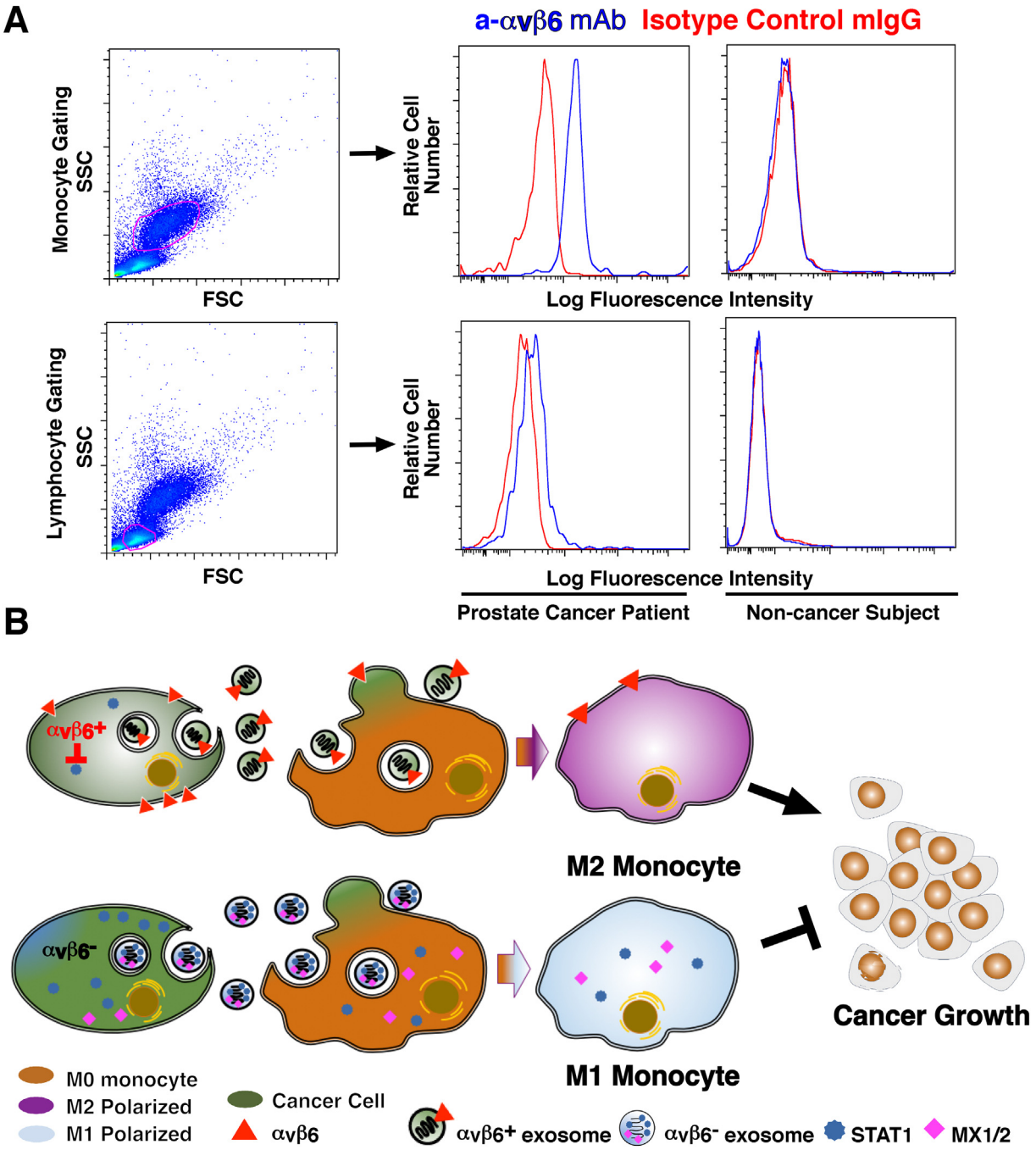

Fig. 7. αvβ6 Integrin is expressed in PBMC from prostate cancer patients. (A), Flow cytometric analysis of αvβ6 expression in PBMC from prostate cancer patients and healthy subjects. Left, monocytes and lymphocytes are gated by SSC and FSC. Right, FACS analysis of αvβ6 cell surface expression in monocytes and lymphocytes from healthy subjects and prostate cancer patients respectively, utilizing 6.3G9 monoclonal antibody to αvβ6 and mouse IgG, as isotype control. Representative data are shown. (B), The schematic diagram shows that transfer of exosomal αvβ6 integrin from prostate cancer cells to monocytes results in down-regulation of STAT1 and MX1/2 levels and increased M2 polarization of monocytes, and has a pro-tumorigenic effect, whereas transfer of αvβ6 integrin–negative exosomes results in increased M1 polarization of monocytes, and inhibits cancer growth.

Please cite this article as: H. Lu, et al., Exosomal αvβ6 integrin is required for monocyte M2 polarization in prostate cancer, Matrix Biol (2017), https://doi.org/10.1016/j.matbio.2018.03.009

MX1/2 levels in cells, exosomes and monocytes will be generated and an anti-tumor effect will be obtained.

Discussion

In this study, we demonstrate that the αvβ6 integrin has profound effects on the microenvironment by preventing induction of the STAT1/MX1/2 signaling pathway in donor cancer cells and their exosomes. In this regard, we show that αvβ6 positive exosomes are transferred to monocytes and promote M2 monocyte polarization, whereas exosomes from cancer cells, in which αvβ6 has been down-regulated or inhibited, carry high levels of STAT1/MX1/2 and inhibit M2. Finally, we demonstrate that αvβ6 inhibition in vivo causes up-regulation of the STAT1 signaling pathway in cancer cells.

The effect of the αvβ6 integrin on STAT1 has significant implications since STAT1 plays a critical role in tumorigenesis by controlling a complex array of activities and functions [53]. In response to cytokines and growth factors, including interferon (IFN)-alpha, IFN-gamma, EGF, PDGF and IL6, STAT1 gets activated by receptor-associated kinases and then forms homo- or heterodimers that translocate to the nucleus and act as transcriptional activators. In many types of tumors, STAT1 induces anti-proliferative genes that directly block tumor growth; it is generally considered as tumor suppressor [54] given its ability to induce immune effector genes which block cell cycle progression [55] or inhibit angiogenesis [56]; in prostate cancer, loss of STAT1 is associated with poor prognosis [57]. In some instances, STAT1 promotes carcinogenesis and tumor survival in particular tissues or as a result of cross-talking with other signaling pathways [58]; however, its dominant effect is likely to promote an anti-tumor immune response given its ability to induce effector expression in immune cells [53]. The effect of αvβ6 integrin on MX1/2 has also significant implications since MX1 expression has been reported to be dependent on STAT1 signaling [59], and MX2, a member of the family of dynamin-like large GTPases, is also interferon-inducible [60] and thus plays a role in the immune response. Only a limited number of studies have examined the role of MX1/2 in cancer [61,62]. MX1 expression has been shown to inversely correlate with prostate cancer and gain of MX1 expression in prostate cancer cells results in cell cycle arrest [61]. Although limited in number, these studies suggest a tumor suppressive role for MX1/2 in prostate cancer. Therefore, by revealing a cross-talk between cancer cells and monocytes mediated by the exosomal αvβ6 and by its inhibitory activity on the STAT1 - MX1/2 pathway, this study indicates that inhibition of this integrin and its downstream effectors might offer a novel immune – based therapeutic strategy in prostate cancer.

Finally, we demonstrate that in the absence of αvβ6, tumor cell exosomes inhibit monocyte M2 polarization. This finding and the knowledge that M2 macrophages are often phenotypically and functionally similar to TAM and support prostate cancer tumorigenicity, provide a strong support for our model (Fig. 7) which illustrates that transfer of integrins, specifically of αvβ6, from cancer cells to monocytes regulates monocyte M2 polarization. The mechanism described here may have wider significance for various types of cancer and may explain how cross-talk between cancer cells and surrounding normal cells, such as leukocytes, may also be mediated by the uptake of exosomal integrins.

Based on our novel mechanistic studies, showing that transfer of exosomes from αvβ6-positive PC3 cells to monocytes drives M2 polarization while transfer of exosomes from αvβ6-negative PC3 cells causes inhibition of M2 polarization, we propose that transfer of integrins, specifically of αvβ6, or integrin–regulated downstream effectors from cancer cells to monocytes promotes prostate cancer progression toward a CRPC phenotype. An additional innovative aspect is that we show for the first time that cancer cell integrins control monocyte response, an area that has begun to be studied; so far, only one study on αvβ3 integrin's role in leukocytes in breast cancer [63] has been published, but a very different mechanism has been proposed since the authors have studied αvβ3 endogenously expressed in leukocytes. Furthermore, since in this study, αvβ3 is shown to have an antitumor effect and promote M1 polarization and STAT1 activation, we can speculate that β6 competes for β3 for binding to the αv subunit and causes a M2 promoting effect. We have reported previously that αvβ6 promotes prostate cancer progression by activation of androgen receptor (AR) in absence of androgen [14]. Androgen blockade in tumor cells, either by castration or MDV 3100 treatment, induces the expression of macrophage colony stimulating factor 1 (CSF-1) and other cytokines, recruits and promotes a M2 phenotype in TAMs [64]. Inhibition of endogenous AR in macrophages results in activation of CCL2/CCR2 and STAT3 and the recruitment of macrophages promotes prostate cancer metastasis [65]. Given the fact that these observations were obtained in androgen blockade setting and αvβ6 promotes a castration resistance mechanism, we may further speculate that the regulatory effect of αvβ6 on prostate cancer is partially mediated by macrophages.

Overall, these studies will pave the way for innovative therapeutic approaches in prostate cancer which will block the transfer, or uptake of αvβ6-containing exosomes, to monocytes. Since it is currently believed that the epithelium-specific αvβ6 integrin functions only in cells that synthesize it, we have now provided evidence for its ability to act

Please cite this article as: H. Lu, et al., Exosomal αvβ6 integrin is required for monocyte M2 polarization in prostate cancer, Matrix Biol (2017), https://doi.org/10.1016/j.matbio.2018.03.009

in cells that do not normally synthesize it. In this context, αvβ6 signaling has been linked to metastasis and bone lesions [18], suggesting that the delivery of this integrin via exosomes may play a role in transferring its related function to monocytes, and that interfering with it, will inhibit CRPC. It may also be speculated that, as for the αvβ3 integrin, the bending and unbending conformational changes of αvβ6 regulated by tensile forces exerted by the exosome structure may affect the vesicle content [66]. As integrins are multifunctional receptors implicated in prostate cancer maintenance, we have shown that their transfer via exosomes from prostate cancer cells to cells in the TME may activate signaling mechanisms important for disease progression. In turn, this may open new therapeutic prospects for patients with advanced, metastatic CRPC, as disruption of integrin-dependent signaling may be expected to inhibit a host of downstream pathways controlling survival mechanisms of protection that promote therapy-resistance. Similarly, a recent study shows that anti-myeloma chemotherapy enhances secretion of tumor cell exosomes, which are rich in heparanase and regulate cytokine expression of macrophages [67]. Future studies will reach a comprehensive mechanistic understanding of integrin-directed signaling in cell-cell communication in prostate cancer progression and open new possibilities for diagnosis and risk stratification, as well as therapy-resistance, in prostate cancer patients [3].

Experimental procedures

Reagents and antibodies (Abs)

Lympholyte®-Mammal (Cedarlane CL5115) was used for the isolation of PBMC and Lympholyte®-Human (Cedarlane CL5015) was used for the isolation of human PBMC. The resulting cell populations demonstrate a high, and non-selective recovery of viable lymphocytes and monocytes. Optiprep (Sigma Aldrich, 1556) was used to generate iodixanol density gradient by ultracentrifugation.

Flow cytometry analysis was performed using the following Abs: mouse monoclonal abs: 6.3G9 against human and mouse αvβ6 integrin from Biogen was described previously [14,29], Alexa Fluor 488® conjugated CD14 (BD Biosciences, 562,689), PE-conjugated CD204 (BD Biosciences, 566,251), APC conjugated CD163 (R&D Systems, 215,927). FITC conjugated rat against mouse IgG (Biolegend, 406,605) was used as a secondary Ab. A rabbit polyclonal Alexa Fluor 488® conjugated F(ab')2 against mouse IgG (Thermo Scientific, A-21204) was used also as a secondary Ab. Purified non-immune mouse IgG (Pierce, 31,903) was used as an isotype control.

The following Abs were used for IB analysis: mouse monoclonal Abs: 6.2A1 against human and mouse αvβ6 (1), CD9 (Santa Cruz, sc18869), CD63 (Abcam, ab8219), CD81 (Abcam, ab23505), MX1/2/3 (Santa Cruz, sc166412). Rabbit polyclonal Abs against: FLOT1 (Abcam, ab41927), TSG101 (Abcam, ab30871), human and mouse STAT1 (Santa Cruz, sc-346), ERK1 (Santa Cruz, sc-93), CANX (Santa Cruz, sc-11,397), actin (Sigma Aldrich, A2066). The same Ab against STAT1 (Santa Cruz, sc-346) was used for immunohistochemistry (IHC) analysis for mouse tissue. Ch2A1 was used for αvβ6 IHC on mouse tumors, as described previously [14].

Control siRNA, D1 and D2 β6 siRNA duplexes (IDT Incorporated) were described previously [14,29].

Cells and culture conditions

PC-3 cells, a prostate cancer cell line and THP-1 cells, a human monocyte cell line were cultured according to American Type Culture Collection recommendations (ATCC). PBMC isolated from mouse and human blood were cultured as previously described [68].

To obtain β6-EGFP PC3 and EGFP-PC3 cell lines, PC3 prostate cancer cells (grown in RPMI supplemented with 10% heat-inactivated FBS and 100 U/mL penicillin) were transfected with EGFP-N3 plasmid (a kind gift from Dr. Fabienne Paumet, Thomas Jefferson University) and used as negative control or β6-EGFP-N3 plasmid having EGFP-tag in the C-terminus of β6-cDNA on plasmid backbone (Addgene plasmid #13593, generated by Dr. Dean Sheppard, UCSF school of medicine, San Francisco, USA) using the Lipofectamine 2000 reagent (Thermo Fisher Scientific) at a ratio of 3 μL Lipofectamine/μg of DNA. Single colonies were obtained by G418 antibiotic selection (1000 μg/mL) and expanded for screening of GFP expression using a fluorescence microscope. Pooled populations of stably transfected cells were generated (β6-EGFP-PC3 and EGFP-PC3) and confirmed for expression of β6-integrin and GFP by IB. The PC3-shβ5 and PC3-shβ6 cells and down-regulation of exosomal β6 Integrin using siRNA duplexes, D1 and D2, or non-specific control siRNA were described previously [69]. PC3-shβ5 transfectants were used as control.

Human samples

Prostate cancer patient ($n = 14$) blood samples were discarded specimens obtained from patients at the Jefferson Medical Oncology Clinic. Age-matched healthy donors ($n = 5$) volunteered to provide samples with written consent documented. All specimens were collected in accordance with a Jefferson IRB approved protocol, coded, and de-identified before processing.

Please cite this article as: H. Lu, et al., Exosomal αvβ6 integrin is required for monocyte M2 polarization in prostate cancer, Matrix Biol (2017), https://doi.org/10.1016/j.matbio.2018.03.009

PBMC isolation

Mouse blood was obtained via cardiac puncture after euthanasia and mixed with Anticoagulant Citrate Dextrose (ACD) Solution (1.4 g citric acid, 2.5 g sodium citrate, 2.0 glucose per 100 mL) at 40 μL ACD per 1 mL blood sample. The anticoagulated blood was diluted with 1 volume of PBS then the mixture was layered over Lympholyte®-Mammal in a ratio of volume 4:3, followed by room temperature centrifugation at 800 g for 30 min without brake. The PBMC containing buffy coat were collected, washed with PBS, and resuspended in complete media for further processing.

PBMC were obtained from EDTA treated human blood following the same methodology, but blood was withdrawn via venipuncture and Lympholyte®-Human was used in a ratio of volume 2:1. Eleven $Pten^{pc-/-}$ mice (52–80 week old) and 9 Pten wild-type mice (40–60 week old) were used for PBMC isolation.

Flow cytometry analysis

Flow cytometric phenotyping of murine and human PBMC was performed as previously described [68]. All flow data were acquired using an LSR ii flow cytometer (BD Biosciences), and were analyzed using FlowJo® software (FlowJo, LLC).

Label-free quantitative analysis by mass spectrometry

Equal amounts of proteins from exosome and cell lysates were run on a 12% SDS gel for 0.5 cm and stained with colloidal blue. Gel lanes were excised and digested with modified trypsin (Promega). Tryptic peptides were analyzed by LC-MS/MS on a Q Exactive Plus mass spectrometer (Thermo Scientific) coupled with a Nano-ACQUITY UPLC system (Waters). Samples were injected onto a UPLC Symmetry trap column (180 μm i.d. × 2 cm packed with 5 μm C18 resin, Waters), and tryptic peptides were separated by RP-HPLC on a BEH C18 nanocapillary analytical column (75 μm i.d. × 25 cm, 1.7 μm particle size, Waters) using a 4 h gradient. Eluted peptides were analyzed by the mass spectrometer set to repetitively scan m/z from 400 to 2000. The full MS scan was collected at 70,000 resolution followed by data-dependent MS/MS scans at 17,500 resolution on the 20 most abundant ions exceeding a minimum threshold of 20,000. Peptide match was set as preferred; exclude isotopes option and charge-state screening were enabled to reject single and unassigned charged ions. MS data were analyzed with MaxQuant 1.5.2.8 software [70]. MS/MS data were searched against the human UniProt protein database (July 2014) using full trypsin specificity with up to two missed cleavages, static carboxamidomethylation of Cys, and variable oxidation of Met, and protein N-terminal acetylation. Consensus identification lists were generated with false discovery rates of 1% at both the protein and peptide levels. For label-free quantitation, the MaxLFQ algorithm was used and the "match between runs" option was enabled to transfer MS/MS identifications across LC-MS/MS runs based on accurate mass and retention time. Unique and razor peptides were considered for quantification and a minimum of two ratio counts were required for each of the normalized protein intensity. Protein tables were filtered to remove reverse database entries, common contaminants, and proteins identified by a single peptide. Normalized intensity data was floored to the minimum detected signal (intensity of 10^7). Unsupervised hierarchical clustering of samples was performed on $\log_{10}$-scaled intensities using normalized Euclidean distance with average linkage. Unpaired two-tail *t*-test was performed between controls (NT, NS) and knockdown (D1, D2) samples and nominal *p*-values were corrected for multiple testing using Benjamini-Hochberg method to estimate False Discovery Rate (FDR). Fold changes were calculated from the mean normalized protein intensities between the two groups. Final list of robustly detected, most changed candidates included affected at least 4 fold, FDR < 10% proteins detected by at least 10 MS/MS counts and at least 10 unique peptides.

Genetically engineered mouse models

$Pten^{pc-/-}$ mice were obtained from UCLA and generated as previously described [71]. The β6-null mice were obtained from Dr. Dean Sheppard, University of California San Francisco [72]. Mice were housed in pathogen-free conditions, and all work was performed in accordance with an IACUC approved protocol, at Thomas Jefferson University.

Exosome isolation

PC3 exosomes were isolated from serum-free cell culture supernatant via ultracentrifugation as described previously [29,48].

For iodixanol gradient separation, a previously described procedure was used [47]. Pellets obtained from ultracentrifugation of conditioned media from PC3 prostate cancer cells were suspended in 1.636 mL of 30% iodixanol solution (made by mixing 1:1 of 60%, wt/vol) stock solution of iodixanol density gradient medium and a buffer (0.25 M sucrose, 10 mM Tris pH 8.0, 1 mM EDTA pH 7.4) and transferred to a SW55Ti rotor tube (Beckman). Next, 0.709 mL of 20% (wt/vol) iodixanol and 0.654 mL of 10% (wt/vol) iodixanol were successively layered on top of the 30% iodixanol-vesicle suspension and tubes were centrifuged for one hour at 350,000 *g* (54,000 rpm), 4 °C, in SW55Ti rotor

Please cite this article as: H. Lu, et al., Exosomal αvβ6 integrin is required for monocyte M2 polarization in prostate cancer, Matrix Biol (2017), https://doi.org/10.1016/j.matbio.2018.03.009

(BECKMAN, L8-70 M Ultracentrifuge). Ten fractions of 0.267 mL were then collected starting from top of the tube. Refractive index was assessed with a refractometer and density calculated. All fractions were diluted with 1 mL PBS and centrifuged for 70 min at 100,000 g (53,000 rpm), 4 °C, in a TLA-100.2 rotor (BECKMAN, Optima TL Ultracentrifuge). The respective pellets thus obtained were washed in 1 mL PBS and again centrifuged for 70 min at 100,000 *g* (53,000 rpm), 4 °C, in a TLA-100.2 rotor. These concentrated fractions were finally resuspended in 30 μL of PBS.

Exosome transfer assays

β6-null PBMC (isolated from 3β6-null mice and pooled) and human normal PBMC, both separated using Lympholyte, or THP1 cells were incubated with or without PC3 derived exosomes. Cells were collected and subjected to IB analysis for β6 levels. To evaluate exosome-mediated internalization of β6, β6-null PBMC were resuspended with sodium acetate buffer (0.2 M acetic acid/0.5 M NaCl, pH 2.8) [14,29] after the incubation with exosomes, then the cells were rinsed with PBS and lysed for IB.

Inhibition assay and immunoblotting analysis

PC3 cells (6.0×10^5) were re-suspended in 3 mL of RPMI1640 medium, supplemented with 10 μg/mL 6.3G9, 1E6 or PBS. Cells were plated into 60 mm tissue culture dishes and incubated for 24 h, and then cells were lysed and the cell lysates were prepared for IB analysis. IB analyses for exosome characterization and β6 integrin expression were performed as previously described [14,29].

Imaging, Ab treatment of *Pten*$^{pc-/-}$ mice and immunohistochemistry analysis

Ab treatment of *Pten*$^{pc-/-}$ Mice has been previously described [14]. Before Ab injection, mouse tumor sizes were measured with the Vevo 2100 high frequency, small animal, ultrasound scanner (Fujifilm/Visualsonics, Toronto, Ontario, Canada) and a 38 MHz linear array transducer (the MS400). The ultrasound scanning was performed by registered sonographer. Tumor volumes were obtained by measuring the lesion dimensions in three orthogonal planes using the build-in calipers on the scanner, and the tumor volume was calculated as Volume = (length×width×height) × Pi/6. Ab treatment of *Pten*$^{pc-/-}$ mice was described previously [14]. IHC was performed on murine formalin-fixed paraffin embedded prostate tumor samples as previously described [14]. Five mice for each group (6.3G9 and 1E6) were analyzed. Stained slides were scored individually.

For each tumor, 3 random invasive adenocarcinoma areas were scanned; the average of the percentage of STAT1 positive neoplastic cells acquired from the 3 areas is shown.

NTA

NTA was performed to characterize exosome samples based on size following a previously established protocol [48] using NS300 (Malvern NanoSight).

Declaration of interest

Paul H. Weinreb is employee and shareholder of Biogen Idec Inc. The other authors have declared that no conflict of interest exists.

Authors' contributions

H. Lu, S. Kurtoglu, C. Fedele, D.C. Hooper, D.W. Speicher, D.C. Altieri and L.R. Languino, designed the study.

H. Lu, N. Bowler, L. Harshyne, S.R. Krishn, S. Kurtoglu, C. Fedele, H. Tang, R. Kean, A. Dutta and Maria Stanczak performed the experiments.

K. Wang acquired blood specimens.

H. Lu, N. Bowler, S. Kurtoglu, L. Harshyne, C. Fedele, H. Tang, P. Fortina and A. Ertel acquired data. H. Lu, N. Bowler, S. Kurtoglu, L. Harshyne, D. C. Hooper, Q. Liu, H. Tang, A.V. Kossenkov, W.K. Kelly, P.H. Weinreb, L. Yu, Flemming Forsberg, D.I. Gabrilovich, D.W. Speicher, D.C. Altieri and L.R. Languino analyzed the data.

P.H. Weinreb provided all antibodies against αvβ6.

H. Lu, S. Kurtoglu, C. Fedele, D.C. Hooper, D.W. Speicher, A.V. Kossenkov, D.C. Altieri and L.R. Languino wrote the manuscript.

Acknowledgements

We are grateful to Dr. S.M. Violette, who provided antibodies against αvβ6; Dr. D. Sheppard who provided β6 knock-out mice; Dr. H. Wu for *Pten*$^{loxp/loxp}$ mice; Amir Yarmahmoodi for support with NTA NS300 (Malvern NanoSight). We are grateful to Veronica Robles for support with the manuscript preparation. For this study, flow cytometry and histology facilities of the Sidney Kimmel Cancer Center, which are supported in part by NCI Cancer Center-Support Grant P30 CA56036, were used.

Funding information

NIH-R01: CA109874 to L.R.L., CA78810 and CA90917 to D.C.A.; NIH-P01 CA140043 to L.R.L., D.C.A., D.I.G and D.W.S.; NIH-R50 CA221838 to H.-Y.T, NIH-R50 CA211199 to A.V.K.; Postdoctoral Research Fellowship from the American Italian Cancer Foundation to C.F. S10 OD010408 to F.F. for support of the ultrasound scanner. This project is also funded, in part, under a Commonwealth University Research Enhancement Program grant with the Pennsylvania Department of Health, SAP# 4100068728 (H.R.); the Department specifically disclaims responsibility for any analyses, interpretations or conclusions.

Appendix A. Supplementary data

Supplementary data to this article can be found online at https://doi.org/10.1016/j.matbio.2018.03.009.

Received 15 February 2018;
Received in revised form 8 March 2018;
Accepted 8 March 2018
Available online xxxx

Keywords:
αvβ6 integrin;
Prostate Cancer;
M2 polarization;
STAT1;
Monocytes;
Exosomes

Current address: Carmine Fedele: Laura and Isaac Perlmutter Cancer Center, NYU Langone Health, New York, NY, 10016, USA.

Current address: Anindita Dutta: TATA Translational Cancer Research Centre, TATA Medical Center, Kolkata, India.

References

[1] R.L. Siegel, K.D. Miller, A. Jemal, Cancer statistics, 2016, CA Cancer J. Clin. 66 (1) (2016) 7–30.
[2] M. Gerlinger, J.W. Catto, T.F. Orntoft, F.X. Real, E.C. Zwarthoff, C. Swanton, Intratumour heterogeneity in urologic cancers: from molecular evidence to clinical implications, Eur. Urol. 67 (4) (2014) 729–737.
[3] A. Alva, M. Hussain, The changing natural history of metastatic prostate cancer, Cancer J. 19 (1) (2013) 19–24.
[4] Z. Culig, Targeting the androgen receptor in prostate cancer, Expert. Opin. Pharmacother. 15 (10) (2014) 1427–1437.
[5] B. Felding-Habermann, Integrin adhesion receptors in tumor metastasis, Clin. Exp. Metastasis 20 (3) (2003) 203–213.
[6] H.L. Goel, J. Li, S. Kogan, L.R. Languino, Integrins in prostate cancer progression, Endocr. Relat. Cancer 15 (3) (2008) 657–664.
[7] K. Hess, C. Boger, H.M. Behrens, C. Rocken, Correlation between the expression of integrins in prostate cancer and clinical outcome in 1284 patients, Ann. Diagn. Pathol. 18 (6) (2014) 343–350.
[8] R.B. Nagle, J.D. Knox, C. Wolf, G.T. Bowden, A.E. Cress, Adhesion molecules, extracellular matrix, and proteases in prostate carcinoma, J. Cell. Biochem. 19 (1994) 232–237.
[9] M. Fornaro, T. Manes, L.R. Languino, Integrins and prostate cancer metastases, Cancer Metastasis Rev. 20 (3–4) (2001) 321–331.
[10] M. Edlund, S.Y. Sung, L.W. Chung, Modulation of prostate cancer growth in bone microenvironments, J. Cell. Biochem. 91 (4) (2004) 686–705.
[11] M. Wirth, A. Heidenreich, J.E. Gschwend, T. Gil, S. Zastrow, M. Laniado, J. Gerloff, M. Zuhlsdorf, G. Mordenti, W. Uhl, H. Lannert, A multicenter phase 1 study of EMD 525797 (DI17E6), a novel humanized monoclonal antibody targeting alphav integrins, in progressive castration-resistant prostate cancer with bone metastases after chemotherapy, Eur. Urol. 65 (5) (2014) 897–904.
[12] D. Bouvard, J. Pouwels, N. De Franceschi, J. Ivaska, Integrin inactivators: balancing cellular functions in vitro and in vivo, Nat. Rev. Mol. Cell Biol. 14 (7) (2013) 432–444.
[13] J. Azare, K. Leslie, H. Al-Ahmadie, W. Gerald, P.H. Weinreb, S.M. Violette, J. Bromberg, Constitutively activated Stat3 induces tumorigenesis and enhances cell motility of prostate epithelial cells through integrin β6, Mol. Cell. Biol. 27 (12) (2007) 4444–4453.
[14] H. Lu, T. Wang, J. Li, C. Fedele, Q. Liu, J. Zhang, Z. Jiang, D. Jain, R.V. Iozzo, S.M. Violette, P.H. Weinreb, R.J. Davis, D. Gioeli, T.J. Fitzgerald, D.C. Altieri, L.R. Languino, αvβ6 integrin promotes castrate-resistant prostate cancer through JNK1-mediated activation of androgen receptor, Cancer Res. 1 (76) (2016) 5163–5174.
[15] D.Q. Zheng, A.S. Woodard, M. Fornaro, G. Tallini, L.R. Languino, Prostatic carcinoma cell migration via αvβ3 integrin is modulated by a focal adhesion kinase pathway, Cancer Res. 59 (7) (1999) 1655–1664.
[16] N.P. McCabe, S. De, A. Vasanji, J. Brainard, T.V. Byzova, Prostate cancer specific integrin αvβ3 modulates bone metastatic growth and tissue remodeling, Oncogene 26 (42) (2007) 6238–6243.
[17] D. Sheppard, Epithelial integrins, BioEssays 18 (8) (1996) 655–660.
[18] A. Dutta, J. Li, H. Lu, J. Akech, J. Pratap, T. Wang, B.J. Zerlanko, T.J. FitzGerald, Z. Jiang, R. Birbe, J. Wixted, S. M. Violette, J.L. Stein, G.S. Stein, J.B. Lian, L.R. Languino, The αvβ6 integrin promotes an osteolytic program through upregulation of MMP2, Cancer Res. 74 (2014) 1598–1608.
[19] K.M. Moore, G.J. Thomas, S.W. Duffy, J. Warwick, R. Gabe, P. Chou, I.O. Ellis, A.R. Green, S. Haider, K. Brouilette, A. Saha, S. Vallath, R. Bowen, C. Chelala, D. Eccles, W.J. Tapper, A.M. Thompson, P. Quinlan, L. Jordan, C. Gillett, A. Brentnall, S. Violette, P.H. Weinreb, J. Kendrew, S.T. Barry, I. R. Hart, J.L. Jones, J.F. Marshall, Therapeutic targeting of integrin αvβ6 in breast cancer, J. Natl. Cancer Inst. 106 (8) (2014).
[20] S. Hazelbag, G.G. Kenter, A. Gorter, E.J. Dreef, L.A. Koopman, S.M. Violette, P.H. Weinreb, G.J. Fleuren,

Overexpression of the αvβ6 integrin in cervical squamous cell carcinoma is a prognostic factor for decreased survival, J. Pathol. 212 (3) (2007) 316–324.
[21] D.I. Cantor, H.R. Cheruku, E.C. Nice, M.S. Baker, Integrin αvβ6 sets the stage for colorectal cancer metastasis, Cancer Metastasis Rev. 34 (4) (2015) 715–734.
[22] H. Hamidi, M. Pietila, J. Ivaska, The complexity of integrins in cancer and new scopes for therapeutic targeting, Br. J. Cancer 115 (9) (2016) 1017–1023.
[23] S. Li, Y. Qi, K. McKee, J. Liu, J. Hsu, P.D. Yurchenco, Integrin and dystroglycan compensate each other to mediate laminin-dependent basement membrane assembly and epiblast polarization, Matrix Biol. 57-58 (2017) 272–284.
[24] T. Hui, E.S. Sorensen, S.R. Rittling, Osteopontin binding to the alpha 4 integrin requires highest affinity integrin conformation, but is independent of post-translational modifications of osteopontin, Matrix Biol. 41 (2015) 19–25.
[25] W.O. Twal, S.M. Hammad, S.L. Guffy, W.S. Argraves, A novel intracellular fibulin-1D variant binds to the cytoplasmic domain of integrin beta 1 subunit, Matrix Biol. 43 (2015) 97–108.
[26] O.M. Viquez, E.M. Yazlovitskaya, T. Tu, G. Mernaugh, P. Secades, K.K. McKee, E. Georges-Labouesse, A. De Arcangelis, V. Quaranta, P. Yurchenco, L.C. Gewin, A. Sonnenberg, A. Pozzi, R. Zent, Integrin alpha6 maintains the structural integrity of the kidney collecting system, Matrix Biol. 57-58 (2017) 244–257.
[27] F. Roche, K. Sipila, S. Honjo, S. Johansson, S. Tugues, J. Heino, L. Claesson-Welsh, Histidine-rich glycoprotein blocks collagen-binding integrins and adhesion of endothelial cells through low-affinity interaction with α2 integrin, Matrix Biol. 48 (2015) 89–99.
[28] A.V. Shinde, R. Kelsh, J.H. Peters, K. Sekiguchi, L. Van De Water, P.J. McKeown-Longo, The α4β1 integrin and the EDA domain of fibronectin regulate a profibrotic phenotype in dermal fibroblasts, Matrix Biol. 41 (2015) 26–35.
[29] C. Fedele, A. Singh, B.J. Zerlanko, R.V. Iozzo, L.R. Languino, The αvβ6 integrin is transferred intercellularly via exosomes, J. Biol. Chem. 290 (8) (2015) 4545–4551.
[30] M. Tkach, J. Kowal, A.E. Zucchetti, L. Enserink, M. Jouve, D. Lankar, M. Saitakis, L. Martin-Jaular, C. Thery, Qualitative differences in T-cell activation by dendritic cell-derived extracellular vesicle subtypes, EMBO J. 36 (20) (2017) 3012–3028.
[31] V.R. Minciacchi, C. Spinelli, M. Reis-Sobreiro, L. Cavallini, S. You, M. Zandian, X. Li, R. Mishra, P. Chiarugi, R.M. Adam, E. M. Posadas, G. Viglietto, M.R. Freeman, E. Cocucci, N.A. Bhowmick, D. Di Vizio, MYC mediates large oncosome-induced fibroblast reprogramming in prostate cancer, Cancer Res. 77 (9) (2017) 2306–2317.
[32] V.R. Minciacchi, M.R. Freeman, D. Di Vizio, Extracellular vesicles in cancer: exosomes, microvesicles and the emerging role of large oncosomes, Semin. Cell Dev. Biol. 40 (2015) 41–51.
[33] H. Peinado, M. Aleckovic, S. Lavotshkin, I. Matei, B. Costa-Silva, G. Moreno-Bueno, M. Hergueta-Redondo, C. Williams, G. Garcia-Santos, C. Ghajar, A. Nitadori-Hoshino, C. Hoffman, K. Badal, B.A. Garcia, M.K. Callahan, J. Yuan, V. R. Martins, J. Skog, R.N. Kaplan, M.S. Brady, J.D. Wolchok, P.B. Chapman, Y. Kang, J. Bromberg, D. Lyden, Melanoma exosomes educate bone marrow progenitor cells toward a pro-metastatic phenotype through MET, Nat. Med. 18 (6) (2012) 883–891.
[34] S.A. Melo, L.B. Luecke, C. Kahlert, A.F. Fernandez, S.T. Gammon, J. Kaye, V.S. LeBleu, E.A. Mittendorf, J. Weitz, N. Rahbari, C. Reissfelder, C. Pilarsky, M.F. Fraga, D. Piwnica-Worms, R. Kalluri, Glypican-1 identifies cancer exosomes and detects early pancreatic cancer, Nature 523 (7559) (2015) 177–182.
[35] R.D. Sanderson, S.K. Bandari, I. Vlodavsky, Proteases and glycosidases on the surface of exosomes: newly discovered mechanisms for extracellular remodeling, Matrix Biol. (2017) https://doi.org/10.1016/j.matbio.2017.10.007 (in press).
[36] Y.H. Song, C. Warncke, S.J. Choi, S. Choi, A.E. Chiou, L. Ling, H.Y. Liu, S. Daniel, M.A. Antonyak, R.A. Cerione, C. Fischbach, Breast cancer-derived extracellular vesicles stimulate myofibroblast differentiation and pro-angiogenic behavior of adipose stem cells, Matrix Biol. 60–61 (2017) 190–205.
[37] A. Hoshino, B. Costa-Silva, T.L. Shen, G. Rodrigues, A. Hashimoto, M. Tesic Mark, H. Molina, S. Kohsaka, A. Di Giannatale, S. Ceder, S. Singh, C. Williams, N. Soplop, K. Uryu, L. Pharmer, T. King, L. Bojmar, A.E. Davies, Y. Ararso, T. Zhang, H. Zhang, J. Hernandez, J.M. Weiss, V.D. Dumont-Cole, K. Kramer, L.H. Wexler, A. Narendran, G.K. Schwartz, J.H. Healey, P. Sandstrom, K. Jorgen Labori, E.H. Kure, P.M. Grandgenett, M.A. Hollingsworth, M. de Sousa, S. Kaur, M. Jain, K. Mallya, S.K. Batra, W.R. Jarnagin, M.S. Brady, O. Fodstad, V. Muller, K. Pantel, A.J. Minn, M.J. Bissell, B.A. Garcia, Y. Kang, V.K. Rajasekhar, C.M. Ghajar, I. Matei, H. Peinado, J. Bromberg, D. Lyden, Tumour exosome integrins determine organotropic metastasis, Nature 527 (7578) (2015) 329–335.
[38] T.M. Beer, E.D. Kwon, C.G. Drake, K. Fizazi, C. Logothetis, G. Gravis, V. Ganju, J. Polikoff, F. Saad, P. Humanski, J.M. Piulats, P. Gonzalez Mella, S.S. Ng, D. Jaeger, F.X. Parnis, F.A. Franke, J. Puente, R. Carvajal, L. Sengelov, M.B. McHenry, A. Varma, A.J. van den Eertwegh, W. Gerritsen, Randomized, double-blind, phase III trial of ipilimumab versus placebo in asymptomatic or minimally symptomatic patients with metastatic chemotherapy-naive castration-resistant prostate cancer, J. Clin. Oncol. 35 (1) (2017) 40–47.
[39] A. Mantovani, A. Sica, S. Sozzani, P. Allavena, A. Vecchi, M. Locati, The chemokine system in diverse forms of macrophage activation and polarization, Trends Immunol. 25 (12) (2004) 677–686.
[40] I. Rhee, Diverse macrophages polarization in tumor microenvironment, Arch. Pharm. Res. 39 (11) (2016) 1588–1596.
[41] A. Petrosyan, S. Da Sacco, N. Tripuraneni, U. Kreuser, M. Lavarreda-Pearce, R. Tamburrini, R.E. De Filippo, G. Orlando, P. Cravedi, L. Perin, A step towards clinical application of acellular matrix: a clue from macrophage polarization, Matrix Biol. 57-58 (2017) 334–346.
[42] T.A. Wynn, A. Chawla, J.W. Pollard, Macrophage biology in development, homeostasis and disease, Nature 496 (7446) (2013) 445–455.
[43] J. Kim, J.S. Bae, Tumor-associated macrophages and neutrophils in tumor microenvironment, Mediat. Inflamm. 2016 (2016) 6058147.
[44] M. Prosniak, L.A. Harshyne, D.W. Andrews, L.C. Kenyon, K. Bedelbaeva, T.V. Apanasovich, E. Heber-Katz, M.T. Curtis, P. Cotzia, D.C. Hooper, Glioma grade is associated with the accumulation and activity of cells bearing M2 monocyte markers, Clin. Cancer Res. 19 (14) (2013) 3776–3786.
[45] A. Sica, M. Erreni, P. Allavena, C. Porta, Macrophage polarization in pathology, Cell. Mol. Life Sci. 72 (21) (2015) 4111–4126.

Please cite this article as: H. Lu, et al., Exosomal αvβ6 integrin is required for monocyte M2 polarization in prostate cancer, Matrix Biol (2017), https://doi.org/10.1016/j.matbio.2018.03.009

[46] J. Zhang, L. Patel, K.J. Pienta, CC chemokine ligand 2 (CCL2) promotes prostate cancer tumorigenesis and metastasis, Cytokine Growth Factor Rev. 21 (1) (2010) 41–48.
[47] J. Kowal, G. Arras, M. Colombo, M. Jouve, J.P. Morath, B. Primdal-Bengtson, F. Dingli, D. Loew, M. Tkach, C. Thery, Proteomic comparison defines novel markers to characterize heterogeneous populations of extracellular vesicle subtypes, Proc. Natl. Acad. Sci. U. S. A. 113 (8) (2016) E968–977.
[48] A. Singh, C. Fedele, H. Lu, M.T. Nevalainen, J.H. Keen, L.R. Languino, Exosome-mediated transfer of αvβ3 integrin from tumorigenic to non-tumorigenic cells promotes a migratory phenotype, Mol. Cancer Res. 14 (11) (2016) 1136–1146.
[49] M. Morin-Brureau, K.M. Hooper, M. Prosniak, S. Sauma, L.A. Harshyne, D.W. Andrews, D.C. Hooper, Enhancement of glioma-specific immunity in mice by "NOBEL", an insulin-like growth factor 1 receptor antisense oligodeoxynucleotide, Cancer Immunol. Immunother. 64 (4) (2015) 447–457.
[50] P. Andersen, M.W. Pedersen, A. Woetmann, M. Villingshoj, M.T. Stockhausen, N. Odum, H.S. Poulsen, EGFR induces expression of IRF-1 via STAT1 and STAT3 activation leading to growth arrest of human cancer cells, Int. J. Cancer 122 (2) (2008) 342–349.
[51] B. Liu, J. Liao, X. Rao, S.A. Kushner, C.D. Chung, D.D. Chang, K. Shuai, Inhibition of Stat1-mediated gene activation by PIAS1, Proc. Natl. Acad. Sci. U. S. A. 95 (18) (1998) 10626–10631.
[52] M. Puhr, J. Hoefer, H. Neuwirt, I.E. Eder, J. Kern, G. Schafer, S. Geley, I. Heidegger, H. Klocker, Z. Culig, PIAS1 is a crucial factor for prostate cancer cell survival and a valid target in docetaxel resistant cells, Oncotarget 5 (23) (2014) 12043–12056.
[53] V. Calo, M. Migliavacca, V. Bazan, M. Macaluso, M. Buscemi, N. Gebbia, A. Russo, STAT proteins: from normal control of cellular events to tumorigenesis, J. Cell. Physiol. 197 (2) (2003) 157–168.
[54] A. Stephanou, D.S. Latchman, STAT-1: a novel regulator of apoptosis, Int. J. Exp. Pathol. 84 (6) (2003) 239–244.
[55] X. Hu, L.B. Ivashkiv, Cross-regulation of signaling pathways by interferon-gamma: implications for immune responses and autoimmune diseases, Immunity 31 (4) (2009) 539–550.
[56] T.E. Battle, R.A. Lynch, D.A. Frank, Signal transducer and activator of transcription 1 activation in endothelial cells is a negative regulator of angiogenesis, Cancer Res. 66 (7) (2006) 3649–3657.
[57] S. Hatziieremia, Z. Mohammed, P. McCall, J.M. Willder, A.K. Roseweir, M.A. Underwood, J. Edwards, Loss of signal transducer and activator of transcription 1 is associated with prostate cancer recurrence, Mol. Carcinog. 55 (11) (2016) 1667–1677.
[58] S. Kusmartsev, D.I. Gabrilovich, STAT1 signaling regulates tumor-associated macrophage-mediated T cell deletion, J. Immunol. 174 (8) (2005) 4880–4891.
[59] D. Holzinger, C. Jorns, S. Stertz, S. Boisson-Dupuis, R. Thimme, M. Weidmann, J.L. Casanova, O. Haller, G. Kochs, Induction of MxA gene expression by influenza A virus requires type I or type III interferon signaling, J. Virol. 81 (14) (2007) 7776–7785.
[60] K. Melen, P. Keskinen, T. Ronni, T. Sareneva, K. Lounatmaa, I. Julkunen, Human MxB protein, an interferon-alpha-inducible GTPase, contains a nuclear targeting signal and is localized in the heterochromatin region beneath the nuclear envelope, J. Biol. Chem. 271 (38) (1996) 23478–23486.
[61] S.G. Brown, A.E. Knowell, A. Hunt, D. Patel, S. Bhosle, J. Chaudhary, Interferon inducible antiviral MxA is inversely associated with prostate cancer and regulates cell cycle, invasion and docetaxel induced apoptosis, Prostate 75 (3) (2015) 266–279.
[62] J.F. Mushinski, P. Nguyen, L.M. Stevens, C. Khanna, S. Lee, E.J. Chung, M.J. Lee, Y.S. Kim, W.M. Linehan, M.A. Horisberger, J.B. Trepel, Inhibition of tumor cell motility by the interferon-inducible GTPase MxA, J. Biol. Chem. 284 (22) (2009) 15206–15214.
[63] X. Su, A.K. Esser, S.R. Amend, J. Xiang, Y. Xu, M.H. Ross, G.C. Fox, T. Kobayashi, V. Steri, K. Roomp, F. Fontana, M.A. Hurchla, B.L. Knolhoff, M.A. Meyer, E.A. Morgan, J.C. Tomasson, J.S. Novack, W. Zou, R. Faccio, D.V. Novack, S.D. Robinson, S.L. Teitelbaum, D.G. DeNardo, J.G. Schneider, K.N. Weilbaecher, Antagonizing integrin beta3 increases immunosuppression in cancer, Cancer Res. 76 (12) (2016) 3484–3495.
[64] J. Escamilla, S. Schokrpur, C. Liu, S.J. Priceman, D. Moughon, Z. Jiang, F. Pouliot, C. Magyar, J.L. Sung, J. Xu, G. Deng, B.L. West, G. Bollag, Y. Fradet, L. Lacombe, M.E. Jung, J. Huang, L. Wu, CSF1 receptor targeting in prostate cancer reverses macrophage-mediated resistance to androgen blockade therapy, Cancer Res. 75 (6) (2015) 950–962.
[65] K. Izumi, L.Y. Fang, A. Mizokami, M. Namiki, L. Li, W.J. Lin, C. Chang, Targeting the androgen receptor with siRNA promotes prostate cancer metastasis through enhanced macrophage recruitment via CCL2/CCR2-induced STAT3 activation, EMBO Mol. Med. 5 (9) (2013) 1383–1401.
[66] Y. Chen, H. Lee, H. Tong, M. Schwartz, C. Zhu, Force regulated conformational change of integrin αVβ3, Matrix Biol. 60–61 (2017) 70–85.
[67] S.K. Bandari, A. Purushothaman, V.C. Ramani, G.J. Brinkley, D.S. Chandrashekar, S. Varambally, J.A. Mobley, Y. Zhang, E.E. Brown, I. Vlodavsky, R.D. Sanderson, Chemotherapy induces secretion of exosomes loaded with heparanase that degrades extracellular matrix and impacts tumor and host cell behavior, Matrix Biol. 65 (2017) 104–118.
[68] L.A. Harshyne, B.J. Nasca, L.C. Kenyon, D.W. Andrews, D. C. Hooper, Serum exosomes and cytokines promote a T-helper cell type 2 environment in the peripheral blood of glioblastoma patients, Neuro-Oncology 18 (2) (2016) 206–215.
[69] A. Dutta, J. Li, C. Fedele, A. Sayeed, A. Singh, S.M. Violette, T.D. Manes, L.R. Languino, αvβ6 integrin is required for TGFβ1-mediated matrix metalloproteinase2 expression, Biochem. J. 466 (3) (2015) 525–536.
[70] J. Cox, M. Mann, MaxQuant enables high peptide identification rates, individualized p.p.b.-range mass accuracies and proteome-wide protein quantification, Nat. Biotechnol. 26 (12) (2008) 1367–1372.
[71] S. Wang, J. Gao, Q. Lei, N. Rozengurt, C. Pritchard, J. Jiao, G.V. Thomas, G. Li, P. Roy-Burman, P.S. Nelson, X. Liu, H. Wu, Prostate-specific deletion of the murine Pten tumor suppressor gene leads to metastatic prostate cancer, Cancer Cell 4 (3) (2003) 209–221.
[72] X.Z. Huang, J.F. Wu, D. Cass, D.J. Erle, D. Corry, S.G. Young, R.V. Farese Jr., D. Sheppard, Inactivation of the integrin beta 6 subunit gene reveals a role of epithelial integrins in regulating inflammation in the lung and skin, J. Cell Biol. 133 (4) (1996) 921–928.

Please cite this article as: H. Lu, et al., Exosomal αvβ6 integrin is required for monocyte M2 polarization in prostate cancer, Matrix Biol (2017), https://doi.org/10.1016/j.matbio.2018.03.009